1-phenyl 2-thiourea (PTU) activates autophagy in zebrafish embryos

Xiang-Ke Chen[a], Joseph Shiu-Kwong Kwan[b], Raymond Chuen-Chung Chang[a,c*] and Alvin Chun-Hang Ma[d*]

[a] Laboratory of Neurodegenerative Diseases, School of Biomedical Sciences, The University of Hong Kong, Pokfulam, Hong Kong, China;

[b] Charing Cross Hospital, Imperial College Healthcare NHS Trust, London, United Kingdom;

[c] State Key Laboratory of Brain and Cognitive Sciences, The University of Hong Kong, Pokfulam, Hong Kong, China

[d] Department of Health Technology and Informatics, Hong Kong Polytechnic University, Hong Kong, China

*Correspondence:

Dr Alvin Chun-Hang MA, PhD

Department of Health Technology and Informatics

Rm. Y924, Lee Shau Kee Building, The Hong Kong Polytechnic University, Hung Hom, Hong Kong

Tel: +852 3400 8913

Fax: +852 2362 4365

Email: alvin.ma@polyu.edu.hk

or

Dr Raymond Chuen-Chung CHANG, PhD

Rm. L4-49, Laboratory Block, Faculty of Medicine Building, 21 Sassoon Road,

Pokfulam, Hong Kong.

Tel: +852 3917-9127

E-mail: rccchang@hku.hk

1-phenyl 2-thiourea (PTU) activates autophagy in zebrafish embryos

1-phenyl 2-thiourea (PTU) is a tyrosinase inhibitor extensively used to block pigmentation and improve optical transparency in zebrafish (*Danio rerio*) embryo. Here, we reported a previously undescribed effect of PTU on autophagy in zebrafish embryos. Upon 0.003% PTU treatment, aberrant autophagosome and autolysosome formation, accumulation of lysosomes and elevated autophagic flux were observed in various tissues and organs of zebrafish embryos, such as skin, brain, and muscle. Similar to PTU treatment, autophagic activation and lysosomal accumulation were also observed in somatic *tyr* mutant zebrafish embryos, which suggest that tyrosinase inhibition may contribute to PTU-induced autophagic activation. Furthermore, we demonstrated that autophagy contributes to pigmentation inhibition, but is not essential to the PTU-induced pigmentation inhibition. With autophagy involves in wide range of physiological and pathological processes and PTU being routinely used in zebrafish research of autophagy-related processes, these observations raise a novel concern in autophagy-related studies using PTU-treated zebrafish embryos.

Abbreviations: 3-MA: 3-methyladenine; Atg: autophagy-related gene; BSA: bovine serum albumin; CHT: caudal hematopoietic tissue; CQ: chloroquine; GFP: green fluorescent protein; hpf: hour-post-fertilization; Lc3: microtubule-associated protein 1 light chain 3; NGS: normal goat serum; PI-3K: type III Phosphatidylinositol 3-kinases; PTU: 1-phenyl 2-thiourea; RFP: red fluorescent protein; sqstm1: sequestosome 1; α-tub: α-tubulin; *tyr*: tyrosinase

Keywords: 1-phenyl 2-thiourea; autophagy; melanogenesis; tyrosinase; zebrafish embryo

Introduction

1-phenyl 2-thiourea (PTU) is an inhibitor of tyrosinase (a vital rate-limiting enzyme for melanogenesis) routinely used for inhibition of pigmentation in zebrafish (*Danio rerio*), in which zebrafish embryos are treated with 0.003% (w/v) (200 μM) PTU before 24 hour-post-fertilization (hpf) to increase their optical transparency for microscopic imaging [1]. Despite several molecular and physiological side effects including altered hatching and survival rate, thyroid function, neural crest development, eye size and visual behaviors were reported over the past decade [2-6], most of the studies still utilize 200 μM PTU to inhibit pigmentation in zebrafish embryos because these known side effects are relatively minimal and only affecting limited research fields. Nevertheless, physiological effects of PTU on zebrafish embryo, which potentially interferes with studies using zebrafish model warrants further investigations.

Macroautophagy/autophagy referred to "self-eating" and is an essential form of cellular reaction to various physiological and pathological conditions, regulating important processes including intracellular materials turnover, cell death, proliferation, development, ageing and tumorigenesis [7]. Loss of vital autophagy-associated genes, such as autophagy-related gene (*Atg)* 5, *Atg7* and *beclin 1 (Becn1)*, result in tumorigenesis, while overexpression of *Atg5* extends lifespan of rodents [8]. Zebrafish models of autophagy, including green fluorescent protein (GFP)-Lc3 (microtubule-associated protein 1 light chain 3) and GFP-gamma-aminobutyric acid A receptor-associated protein (Gabarap) transgenic zebrafish, as well as autophagy-related genes (*atgs*) knockdown or knockout models, were gradually established in the past decade [9-10] for a broad range of physiological and pathological studies, including

organogenesis, regeneration, and infection [11-13]. Taking the advantage of optical transparency, live imaging with PTU treatment to suppress pigmentation is conventionally applied to study autophagy *in vivo* with transgenic zebrafish embryos, which cannot be conducted in rodent models.

Previous studies demonstrated that autophagy modulates both melanogenesis and melanosome destruction, particularly in melanocytes [14-15]. Knockdown of *LC3*, one of the key autophagic proteins, inhibits melanogenesis in melanocytes [16]. Moreover, several melanogenic inhibitors, such as ARP101, resveratrol, and Hinokitiol, block pigmentation via autophagy-dependent pathways in melanocytes [17-19]. While these previous studies mainly focused on how melanogenesis is regulated through autophagy using *in vitro* melanocyte models, the effects of melanogenic modulators on autophagy remain unclear, particularly at whole-organism level. Here, we report a previously undescribed induction effect of PTU treatment on autophagy in zebrafish embryos, which should be taken into consideration when applying PTU-treated zebrafish embryos in autophagy-related studies.

Results

1-phenyl 2-thiourea (PUT) induces autophagy in zebrafish embryos.

Upon treatment with 0.003% PTU shortly before 24 hpf, optically clear zebrafish embryos were obtained (**Fig. 1A**). To study the autophagic activity in PTU-treated zebrafish embryos, zebrafish embryos were treated with a gradient concentration of PTU from 1X (0.003%), 2X (0.006%) up to 4X (0.012%). Western blot results showed

that both Lc3-I and Lc3-II increased significantly under PTU treatments compared with control in a dose-dependent manner. sqstm1 (sequestosome 1), as a conventional autophagy marker, also decreased significantly in 2X- and 4X-treatment compared with control (**Fig. 1B**), indicated the increased expression of Lc3 protein and autophagosome and/or autolysosome formation [20]. We further investigated autophagosome and/or autolysosome formation using Tg(GFP-Lc3) zebrafish embryos stained with LysoTracker Red, a fluorescent probe labeling lysosome and autolysosome after autophagosome-lysosome fusion. Consistent with western blot results, GFP-Lc3+ (autophagosome and/or autolysosome), LysoTracker+ (lysosome), and GFP-Lc3+ and LysoTracker+ (Merged, autolysosome) puncta increased in PTU-treated neurons in a dose-dependent manner (**Fig. S1A**). Moreover, GFP-Lc3+, LysoTracker+, and GFP-Lc3+ and LysoTracker+ puncta also increased significantly in skin cells, muscle cells and cells in caudal hematopoietic tissue (CHT) of PTU-treated embryos compared with control (**Fig. 1C; Fig. S1B**). The increased GFP-Lc3+ puncta, and GFP-Lc3+ and LysoTracker+ puncta under PTU treatment could be alleviated by 3-methyladenine (3-MA) treatment (**Fig. 1D**), an inhibitor of autophagosome formation via blockage of PI-3K (type III Phosphatidylinositol 3-kinases), suggested that PTU activated autophagy targeting upstream of PI-3K. Collectively, 0.003% PTU treatment shortly before 24 hpf induced autophagic activation characterized by increase in autophagosome, lysosome, and autolysosome in various tissues of zebrafish embryos. Similar autophagic activation was also observed in zebrafish embryos treated with 0.003% PTU at 48 hpf after pigment formation (data not shown).

1-phenyl 2-thiourea (PTU) increases autophagic flux in zebrafish embryos.

We next investigated if PTU treatment accelerates autophagic flux using the GFP-LC3-red fluorescent protein (RFP)-LC3ΔG probe. GFP-LC3 in the probe will be degraded by autophagy while RFP-LC3ΔG remained as internal control and therefore, GFP to RFP fluorescent signal ratio will represent the rate of autophagic flux [21]. In PTU-treated embryos, GFP to RFP signal ratio decreased significantly in skin (**Fig. 2A**). At higher magnification, increased number of GFP-RFP+, and GFP+RFP+ puncta were observed in midbrain cells (**Fig. 2B; Fig. S1C**), indicated the increase of autophagic flux after PTU treatment. Chloroquine (CQ) was also applied to block the fusion of autophagosome with lysosome and subsequent degradation. While CQ treatment alone did not alter Lc3-II:α-tubulin (α-tub) ratio compared with control as shown by western blot, PTU and CQ co-treatment significantly increased the ratio compared with PTU treatment alone (**Fig. 2C**). The relative number of GFP-Lc3+ and LysoTracker- puncta (autophagosome) also increased significantly in neurons in midbrain of Tg(GFP-Lc3) zebrafish embryos in CQ+PTU co-treatment (379%) and CQ treatment alone (199%) compared with PTU (153%) and control (100%), respectively (**Fig. 2D**). The significantly higher fold-increase in autophagosome after CQ co-treatment in PTU-treated embryos (2.59 fold) compared with control (1.99 fold) further demonstrated that PTU treatment elevated autophagic flux. As expected, the number of GFP-Lc3+ and LysoTracker+ puncta (autolysosome) declined significantly and the number of GFP-Lc3- and LysoTracker+ puncta (lysosome) remained unchanged in both control and PTU-treated embryos after CQ treatment (**Fig. 2D**).

Genetic targeting of tyrosinase also induces autophagy in zebrafish embryos.

Tyrosinase, the vital regulatory enzyme underlying PTU-induced anti-melanogenesis, was expressed not only in melanocytes but various organs and tissues of zebrafish

embryos, such as skin, eye, brain, muscle and CHT, and the expression level declined after PTU treatment (**Fig. S2A and B**). To determine whether tyrosinase inhibition is the mechanism underlying PTU-induced autophagy, we targeted tyrosinase (*tyr*) in zebrafish embryos using clustered regularly interspaced short palindromic repeats (CRISPR)-Cas9 as described previously [22]. Optically clear *tyr* gRNA-injected (F0) zebrafish embryos (referred herein as tyr^{Mut}) were generated by injecting *tyr* gRNA together with Cas9 protein (**Fig. 3A**). Western blot result showed that the Lc3-II:α-tub ratio increased significantly in tyr^{Mut} compared with control (**Fig. 3B**). A similar elevated expression of Lc3 protein was also observed in commonly used transparent mutant lines, *Casper* (*roy*^{a9}; *mitfa*^{w2}) and *Absolute* (*ennrba*^{b140}; *mitfa*^{b692}) zebrafish embryos (**Fig. S2C and D**). The number of GFP-Lc3+, LysoTracker+, and GFP-Lc3+ and LysoTracker+ puncta in skin cells and neurons of Tg(GFP-Lc3) embryo co-stained with LysoTracker increased significantly in tyr^{Mut} compared with control, suggested that *tyr* mutation elicited the formation of autophagosome, lysosome, and autolysosome (**Fig. 3C and D**). We further examined the autophagy activities in tyr^{Mut} with autophagy inhibitors. 3-MA treatment significantly decreased the number of GFP-Lc3+ puncta in tyr^{Mut} neurons (**Fig. S3**), demonstrated that *tyr* mutation also activates autophagy upstream of PI-3K similar to PTU treatment. In addition, CQ co-treatment also significantly increased the number of GFP-Lc3+ and LysoTracker- puncta while decreased the number of GFP+ and LysoTracker+ puncta (**Fig 3D**). However, no significant change was observed in the fold-increase of GFP-Lc3+ and LysoTracker- puncta after CQ co-treatment in tyr^{Mut} (1.57 fold) compared with control (1.79 fold). These results indicated that autophagy flux was not elevated in tyr^{Mut}, which was also supported by western blot result that the CQ treatment-induced increase in Lc3-II:α-tub ratio was similar in tyr^{Mut} compared with control (**Fig. 3B**). While the discrepancies

observed between PTU-treated embryos and tyr^{Mut} might due to incomplete and mosaic *tyr* targeting in somatic tyr^{Mut}, genetic inhibition of *tyr* did recapitulate PTU-induced increase in autophagosome and autolysosome formation in zebrafish embryos. Also, PTU co-treatment failed to elicit a higher level of autophagic activation in tyr^{Mut} (**Fig. S3**), suggested that PTU-induced autophagy activity was likely specific to tyrosinase-inhibition.

Autophagy is not essential to 1-phenyl 2-thiourea (PTU)-induced anti-melanogenesis.

Since PTU is a robust tyrosinase inhibitor routinely used to block the production of melanin in zebrafish embryo, we subsequently investigated whether the pigmentation inhibition effects of PTU is autophagy-dependent. While autophagy inhibitors (CQ and 3-MA) had no observable effect on pigmentation, Rapamycin, a conventional autophagic activator targeting mTOR (mechanistic target of rapamycin), reduced pigmentation in zebrafish embryos with significant enhanced autophagic activities (**Fig. 4A; Fig. S3**). Furthermore, blockage of PTU-induced autophagic activity by CQ and 3-MA failed to rescue pigmentation in zebrafish embryos (**Fig. 1D; Fig. 2D; Fig. 4A**). These results suggested that while Rapamycin-induced autophagy contributes to pigmentation inhibition, autophagy is not essential to PTU-induced anti-melanogenesis in zebrafish embryos. Interestingly, L-tyrosine, a key substrate of melanogenic pathway, could partially restore pigmentation in PTU-treated zebrafish embryos (**Fig. 4A**). In addition, L-tyrosine treatment did not ameliorate PTU-induced autophagic activity but induced autophagic activity in both control and PTU-treated embryos (**Fig. 4B**), suggested that L-tyrosine may participate in PTU-induced autophagy and anti-melanogenesis.

Discussion

Zebrafish has emerged rapidly as an *in vivo* model of multiple physiological and pathological processes, including autophagy and its relevant pathways [23]. An optically clear body during embryonic stages facilitates the visualization of transgenic zebrafish lines labelled with fluorescent proteins under microscope [10]. To maintain the transparency of zebrafish during embryogenesis, 0.003% PTU treatment has been widely used as standard strategy of pigmentation inhibition. Although several side effects of PTU treatment on zebrafish embryos have been shown, these side effects are not sufficient to cease the use of PTU in zebrafish research [2-6].

Here, we first reported that PTU treatment induces dose-dependent aberrant autophagosome, lysosomes and autolysosomes formation as well as elevated autophagic flux in various tissues and organs of zebrafish embryos, indicating that PTU-induced autophagy is not specific to melanocytes or surrounding skin cells. In PTU-treated embryos, both Lc3-I and Lc3-II increased significantly, indicated the concomitant increase in Lc3 expression and conversion of Lc3-I to Lc3-II, which is consistent with previously reported autophagy induction in rapamycin-treated zebrafish embryo [9,24]. We further demonstrated that inhibition of tyrosinase via genetic manipulation also induces aberrant autophagosome, lysosomes and autolysosomes formation while PTU co-treatment failed to elicit a higher level of autophagic activation in tyrosinase mutant embryos. Although autophagy flux was not elevated in tyr^{Mut}, which might due to incomplete and mosaic targeting of tyrosinase in somatic tyr^{Mut}, PTU-induced autophagy and accumulation of lysosome are likely specific to tyrosinase inhibition.

Tyrosinase as one of key enzymes in melanogenesis has been described to express predominantly in melanocytes, although it is also detected in various tissues and organs of human and mice [25-26]. In zebrafish embryo, we showed that tyrosinase also expressed in skin, brain as well as muscle cells and PTU treatment suppressed tyrosinase at protein level. While the function of tyrosinase outside melanocyte remains unknown, these results provide an explanation for the PTU-induced autophagy and lysosome accumulation observed in tissues other than melanocytes and skin.

Our findings also demonstrated that autophagy is not essential to PTU-induced anti-melanogenesis effects, though rapamycin-induced autophagy contributes to pigmentation inhibition. A previous study has reported that PTU treatment inhibited tyrosinase activity and degraded tyrosinase protein following Golgi maturation in melanocytes [27]. It is possible that autophagy participates in degradation of non-functional tyrosinase but not inhibition of tyrosinase, and thus, autophagic inhibitors cannot restore tyrosinase activity and melanogenesis in PTU-treated zebrafish embryos. A recent study revealed that knockdown of *LC3* and rapamycin treatment declined and enhanced tyrosinase activity, respectively, demonstrated that autophagy might be essential for the maintenance of tyrosinase level during melanogenesis [16].

Besides the increased number of autophagosome and autolysosome, PTU treatment also pronouncedly increased the number of lysosome. Since tyrosinase can be mistargeted to lysosomes for degradation [28], extra lysosome formation might be induced for non-autophagy removal of tyrosinase under PTU treatment. In addition, tyrosinase catalyzes the oxidation of tyrosine mainly in lysosomes (or

premelanosomes) during melanogenesis [29], it is possible that a feedback mechanism also contributes to the accumulation of lysosome.

In our study, we also found that L-tyrosine treatment partially restored pigmentation in PTU-treated embryos without ameliorating PTU-induced autophagic activity and L-tyrosine treatment alone also induced autophagic activity. While L-tyrosine can directly enhance tyrosinase activity [30], which might contribute to the rescue of pigmentation, the corresponding sub-cellular mechanism underlying L-tyrosine-induced autophagy remains further investigation. It is possible that autophagy contributes to pigmentation through turnover of tyrosinase substrates (L-tyrosine) or the excess nutrient condition (excess L-tyrosine) induces autophagy through reactive oxygen species (ROS)-mediated endoplasmic reticulum (ER) stress signalling independent of mechanistic target of rapamycin pathway [31-32]. While previous study revealed that autophagy plays opposite roles in melanogenesis in melanocytes and keratinocytes [33], the precise role of autophagy in melanin synthesis and deconstruction, particularly melanosome degradation in non-melanocyte cell warrants further investigation.

Since autophagy implicates in wide range of physiological and pathological processes, including cancer, our observations raise a novel concern in autophagy-related studies using PTU-treated zebrafish embryos. Although previous zebrafish studies mostly compared control and treated zebrafish embryos underwent the same PTU treatment, the synergistic or masking effects between PTU and other experimental treatments might still affect the interpretation of autophagy and autophagy-related phenotypes. As one of the most evolutionarily conserved pathways, anti-melanogenesis induced by PTU treatment and genetic modification in melanogenesis-related genes have also been

used in other animal models including rodents and *Xenopus* [34-36]. Therefore, further research on potential anti-melanogenesis-induced autophagy in other animal models is also in need.

Various transparent transgenic zebrafish lines, including *Casper* (*roy*^{a9}; *mitfa*^{w2}) and *Absolute* (*ennrba*^{b140}; *mitfa*^{b692}) were reported in recent years to substitute PTU treatment [37]. However, our results demonstrated that genetic targeting of *tyr* also resulted in aberrant formation of autophagosome, lysosome and autolysosome. Our observation that Lc3 protein level increased in homozygous *Casper* and *Absolute* mutant embryos suggesting that these transparent lines might not represent a better alternative to PTU-treatment. Instead, using better microscopic system, for example, the Lightsheet Microscope used in this study, *in vivo* fluorescent imaging on autophagy signal could be performed and image quality are only minimally affected by pigments on live zebrafish embryos. Nevertheless, these limitations should not obscure the unique advantages of zebrafish model in autophagy-related research.

Materials and Methods

Zebrafish strains and maintenance.

Wild-type and transgenic zebrafish strains were maintained under standard conditions (14:10 h light:dark cycle and fed living brine shrimp twice a day). *Casper* (*roy*^{a9}; *mitfa*^{w2}) and Tg(GFP-Lc3) zebrafish were a generous gift from Dr. S.H. Cheng, City University of Hong Kong, HK and Dr. X. Xu, Mayo Clinic, US, respectively. *Absolute* (*ennrb1a*^{b140}; *mitfa*^{b692}) zebrafish were purchased from Zebrafish International Resource Center (ZIRC). Zebrafish embryos were collected from natural spawning and raised at 28.5°C. Embryo and larvae were staged by hours post fertilization (hpf) and

morphological criteria previously described [38]. All animal experiments were conducted in accordance with protocols approved by the Committee of the Use of Laboratory and Research Animals (CULATR) of the University of Hong Kong and Animal Subjects Ethics Sub-Committee (ASESC) of The Hong Kong Polytechnic University.

Generation of tyrosinase mutant (*$\mathbf{tyr^{Mut}}$*) fish by CRISPR-Cas9.

Tyrosinase (*tyr*) single guide RNA (sgRNA) was synthesized by cloning a 20-base pair (bp) coding sequence 5'-GGGCCGCAGTATCCTCACTC-3' into the pT7-gRNA vector (Addgene, 46759; Wenbiao Chen Lab), which was subsequently linearized with BamH1-HF (New England Biolabs, R3136) and *in vitro* transcribed using HiScribe 376 T7 Quick High Yield RNA synthesis kit (New England Biolabs, E2050S) as previously described [22]. Alt-R S.p. Cas9 Nuclease 3NLS (Integrated DNA Technologies, 1074181) diluted in Cas9 working buffer (20 mM HEPES, 150 mM KCl, pH 7.5) was applied in this study. For microinjection, equal volumes of folded *tyr* sgRNA (100 ng/μL) and Cas9 Nuclease (500 ng/μL) were assembled by incubating at 37°C for 10 min and co-injected into one-cell-stage zebrafish embryos.

Synthesis of GFP-LC3-RFP-LC3ΔG florescent probe.

pMRX-IP-GFP-LC3-RFP-LC3ΔG (Addgene, 84572; Noboru Mizushima Lab) [21] was digested by BglII (New England Biolabs, R0144) and NotI (New England Biolabs, R3189), GFP-LC3-RFP-LC3ΔG then was sub-cloned into BglII and EcoRv (New England Biolabs, R0195) pre-digested pT3TS vector (Addgene, 31830; Stephen Ekker Lab) through Gibson Assembly using ClonExpress Ultra One Step Cloning Kit (Vazyme Biotech, C115) in accordance to manufacturer's instructions. GFP-LC3-RFP-

LC3ΔG mRNA was generated by *in vitro* transcribed using mMESSAGE mMACHINE™ T3 Transcription Kit (Invitrogen; AM1348) and then polyadenylated with the Poly(A) Tailing Kit (Invitrogen; AM1350). After purification, 500 pg GFP-LC3-RFP-LC3ΔG mRNA was injected into the yolk of one-cell-stage zebrafish embryos.

1-phenyl 2-thiourea treatment.

Zebrafish embryos were transferred into Petri dishes with 0.003% PTU (Sigma-Aldrich, P7629) in E3 medium (5 mM NaCl, 0.17 mM KCL, 0.33 mM CaCl, and 0.33 mM $MgSO_4$ at pH 7.4) shortly before 24 hpf to inhibit pigmentation. For dose-dependent trial, a gradient concentration of PTU was applied, including 0.00% PTU (0X), 0.003% PTU (1X), 0.006% PTU (2X), and 0.012% PTU (4X). In addition, for imaging 24 hpf zebrafish embryo, embryos were transferred into Petri dishes with 0.003% PTU in E3 medium at around 6 hpf.

Autophagic modulators and L-tyrosine treatment.

Zebrafish embryos were incubated with 20 μM rapamycin (Selleckchem, S1039), 5 mM 3-methyladenine (Selleckchem, S2767) and 50 μM chloroquine (Selleckchem, S4157) [10], and 5 mM l-tyrosine disodium salt hydrate (Sangon Biotech, A606792) diluted in E3 medium with or without 0.003% PTU from 48 hpf to 96 hpf with solutions refreshed daily.

Western blotting.

Dechorionated and deyolked embryos were homogenized in cell lysis buffer (Sigma-Aldrich, C3228). Embryo lysates mixed with 5X sodium dodecyl sulfate (SDS) loading

buffer (250 mM Tris-HCl, pH 6.8, 10% sodium dodecyl sulfate, 30% glycerol, 0.02% bromophenol blue, 5% β-Mercaptoethanol) were boiled at 95°C for 5 min and then resolved on 12% gels and transferred to the membrane. After blocking with 5% nonfat dried milk for 2 h at room temperature, membranes were probed with Anti-LC3B (Abcam, ab48394), Anti-SQSTM1/p62 (Cell Signalling Technology, 5114) and Anti-alpha Tubulin (Abcam, ab15246) primary antibodies at 4°C overnight. Afterward, the membrane was washed with Tris-buffered saline (50 mM Tris base, 150 mM NaCl, pH 7.5) plus Tween-20 (TBST) and incubated with Goat anti-rabbit IgG secondary antibody (Invitrogen, 32460) for 2 h at room temperature. Membrane was then washed with TBST and visualized using SuperSignal™ West Femto Maximum Sensitivity Substrate (Thermo Fisher, 34095) following the manufacturer's instructions.

LysoTracker Red staining.

LysoTracker Red DND-99 (Invitrogen, L7528) was diluted in E3 medium to a final concentration at 10 μM. 96 hpf embryos were then transferred into the prewarmed diluted dye and incubated at 28.5°C in dark for 45 min in accordance with the protocol previously described [39-40]. Subsequently, embryos were rinsed 4 times with 1 ml fresh E3 medium before imaging.

Confocal Microscope and Lightsheet Microscope and imaging.

Zebrafish embryos were anesthetized using 0.16 mg/ml tricaine (Sigma-Aldrich, A5040), and then mounted in 1.5% low-melting agarose (Sigma-Aldrich, A9045) into 35 mm glass-bottom confocal dish and glass capillary for confocal and lightsheet imaging, respectively. Leica TCS SPE Confocal Microscope was applied to take images with the 10x and 40x objective lenses, while Zeiss Lightsheet Z.1 Selective

Plane Illumination Microscope (LSFM) was used to image with a 20X objective lens. In addition, morphology and pigmentation of zebrafish embryos were imaged by using the Nikon Stereomicroscope with a Nikon DS-Fi2 Camera.

Quantitative analysis and statistics.

Mean fluorescent intensity of specific fluorescence channel imaged using Lightsheet Microscope was measured in the same area of skin above head by using Zeiss ZEN software to quantify the ratio of GFP-LC3 to RFP-LC3ΔG for autophagic flux. The relative number of GFP-Lc3+ (autophagosome and/or autolysosome), GFP-Lc3+ and LysoTracker- (autophagosome), LysoTracker+ puncta (lysosome), and GFP-Lc3+ and LysoTracker+ (Merged, autolysosome) puncta per cell were counted in maximally projected Z-Stack (10 layers out of 100 layers) images of neurons in midbrain, muscle cells in the trunk, maximally projected Z-Stack (100 layers) of cells in CHT. Puncta was defined by fluorescence signals occupy more than one pixel that was distinguished from background signal as previously described [41]. Total number of puncta in at least ten independent cells were counted for each sample and the number of puncta per cell was calculated using total number of puncta divided by the number of cell. ImageJ (NIH) was applied for quantitation of western blot results. Data are presented as mean ± standard deviation (S.D.). Statistical analyses were performed where appropriate using Statistical Package for the Social Sciences (SPSS) Version 14.0 and a p-value less than 0.05 was considered statistically significant.

Disclosure statement

No potential conflicts of interest were disclosed.

Funding

This work is supported by the FHB HMRF [03143765] and FHB HMRF [06173226] to ACM.

Acknowledgement

The zebrafish maintenance was supported by Fish Model Translational Research Laboratory (HTI, PolyU) and Faculty Core Facility (LKS Faculty of Medicine, HKU). Confocal imaging was taken in University Research Facility in Life Sciences (ULS, PolyU) with the help from Dr. Clara Hung.

References

1. Westerfield M. The zebrafish book: a guide for the laboratory use of zebrafish (Danio rerio). University of Oregon Press, Eugene. 2007.
2. Karlsson J, von Hofsten J, Olsson PE. Generating transparent zebrafish: a refined method to improve detection of gene expression during embryonic development. Marine Biotechnology (NY). 2001;3(6):522-527.
3. Elsalini OA, Rohr KB. Phenylthiourea disrupts thyroid function in developing zebrafish. Development genes and evolution. 2003;212(12):593-598.
4. Bohnsack BL, Gallina D, Kahana A. Phenothiourea sensitizes zebrafish cranial neural crest and extraocular muscle development to changes in retinoic acid and IGF signaling. PLoS One. 2011;6(8):e22991.
5. Li Z, Ptak D, Zhang L, et al. Phenylthiourea specifically reduces zebrafish eye size. PLoS One. 2012;7(6):e40132.
6. Antinucci P, Hindges R. A crystal-clear zebrafish for in vivo imaging. Scientific Reports. 2016;6:29490.
7. Levine B, Kroemer G. Autophagy in the pathogenesis of disease. Cell. 2008;132(1):27-42.
8. Choi AM, Ryter SW, Levine B. Autophagy in human health and disease. New England Journal of Medicine. 2013;368(7):651-662.
9. He C, Bartholomew CR, Zhou W, et al. Assaying autophagic activity in transgenic GFP-Lc3 and GFP-Gabarap zebrafish embryos. Autophagy. 2009;5(4):520-526.
10. Varga M, Fodor E, Vellai T. Autophagy in zebrafish. Methods. 2015;75:172-180.
11. Hu Z, Zhang J, Zhang Q. Expression pattern and functions of autophagy-related gene atg5 in zebrafish organogenesis. Autophagy. 2011;7(12):1514-1527.

12. Varga M, Sass M, Papp D, et al. Autophagy is required for zebrafish caudal fin regeneration. Cell Death and Differentiation. 2014;21(4):547-556.
13. Mostowy S, Boucontet L, Mazon Moya MJ, et al. The zebrafish as a new model for the in vivo study of Shigella flexneri interaction with phagocytes and bacterial autophagy. PLoS Pathogens. 2013;9(9):e1003588.
14. Ganesan AK, Ho H, Bodemann B, et al. Genome-wide siRNA-based functional genomics of pigmentation identifies novel genes and pathways that impact melanogenesis in human cells. PLoS Genetics. 2008;4(12):e1000298.
15. Ho H, Ganesan AK. The pleiotropic roles of autophagy regulators in melanogenesis. Pigment Cell & Melanoma Research. 2011;24(4):595-604.
16. Yun WJ, Kim EY, Park JE, et al. Microtubule-associated protein light chain 3 is involved in melanogenesis via regulation of MITF expression in melanocytes. Scientific Reports. 2016;6:19914.
17. Kim ES, Chang H, Choi H, et al. Autophagy induced by resveratrol suppresses α-MSH-induced melanogenesis. Experimental Dermatology. 2014;23(3):204-206.
18. Kim ES, Jo YK, Park SJ, et al. ARP101 inhibits α-MSH-stimulated melanogenesis by regulation of autophagy in melanocytes. FEBS Letters. 2013;587(24):3955-3960.
19. Tsao YT, Huang YF, Kuo CY, et al. Hinokitiol inhibits melanogenesis via AKT/mTOR signaling in B16F10 mouse melanoma cells. International Journal of Molecular Sciences. 2016;17(2):248.
20. Klionsky DJ, Abdelmohsen K, Abe A, et al. Guidelines for the use and interpretation of assays for monitoring autophagy. Autophagy. 2016;12(1):1-222.
21. Kaizuka T, Morishita H, Hama Y, et al. An autophagic flux probe that releases an internal control. Molecular Cell. 2016;64(4):835-849.

22. Ata H, Ekstrom TL, Martínez-Gálvez G, et al. Robust activation of microhomology-mediated end joining for precision gene editing applications. PLoS Genetics. 2018;14(9):e1007652.

23. Lieschke GJ, Currie PD. Animal models of human disease: zebrafish swim into view. Nature Reviews Genetics. 2007;8(5):353-367.

24. Espín-Palazón R, Martínez-López A, Roca FJ, et al. TNFα impairs rhabdoviral clearance by inhibiting the host autophagic antiviral response. PLoS Pathogens. 2016;12(6):e1005699.

25. Abattyani Z, Xerri L, Hassoun J, et al. Tyrosinase gene expression in human tissues. Pigment Cell Research. 1993;6(6):400-405.

26. Tief K, Schmidt A, Beermann F. New evidence for presence of tyrosinase in substantia nigra, forebrain and midbrain. Molecular Brain Research. 1998;53(1-2):307-310.

27. Hall AM, Orlow SJ. Degradation of tyrosinase induced by phenylthiourea occurs following Golgi maturation. Pigment Cell Research. 2005;18(2):122-129.

28. Fujita H, Motokawa T, Katagiri T, et al. Inulavosin, a melanogenesis inhibitor, leads to mistargeting of tyrosinase to lysosomes and accelerates its degradation. Journal of Investigative Dermatology. 2009;129(6):1489-1499.

29. Sánchez-Ferrer Á, Rodríguez-López JN, García-Cánovas F, et al. Tyrosinase: a comprehensive review of its mechanism. Biochimica et Biophysica Acta (BBA)-Protein Structure and Molecular Enzymology. 1995;1247(1):1-11.

30. Slominski A, Zmijewski MA, Pawelek J. L‐tyrosine and L‐dihydroxyphenylalanine as hormone‐like regulators of melanocyte functions. Pigment Cell & Melanoma Research, 2012;25(1):14-27.

31. Ma T, Zhu J, Chen X, et al. High glucose induces autophagy in podocytes. Experimental Cell Research. 2013;319(6):779-789.

32. Yao J, Tao ZF, Li CP, et al. Regulation of autophagy by high glucose in human retinal pigment epithelium. Cellular Physiology and Biochemistry. 2014;33(1):107-116.

33. Murase D, Hachiya A, Takano K, et al. Autophagy has a significant role in determining skin color by regulating melanosome degradation in keratinocytes. Journal of Investigative Dermatology. 2013;133(10):2416-2424.

34. Dieke SH. Pigmentation and hair growth in black rats, as modified by the chronic administration of thiourea, phenyl thiourea and alpha-naphthyl thiourea. Endocrinology. 1947;40(3):123-136.

35. Millott N, Lynn WG. Ubiquity of melanin and the effect of phenylthiourea. Nature. 1966;209(5018):99-101.

36. Steingrímsson E, Copeland NG, Jenkins NA. Melanocyte stem cell maintenance and hair graying. Cell. 2005;121(1):9-12.

37. White RM, Sessa A, Burke C, et al. Transparent adult zebrafish as a tool for in vivo transplantation analysis. Cell Stem Cell. 2008;2(2):183-189.

38. Kimmel CB, Ballard WW, Kimmel SR, et al. Stages of embryonic development of the zebrafish. Developmental Dynamics. 1995;203(3):253-310.

39. He C, Klionsky DJ. Analyzing autophagy in zebrafish. Autophagy. 2010;6(5):642-644.

40. Sasaki T, Lian S, Qi J, et al. Aberrant autolysosomal regulation is linked to the induction of embryonic senescence: differential roles of Beclin 1 and p53 in vertebrate Spns1 deficiency. PLoS Genetics. 2014;10(6):e1004409.

41. Khuansuwan S, Barnhill LM, Cheng S, et al. A novel transgenic zebrafish line allows for in vivo quantification of autophagic activity in neurons. Autophagy. 2019;15(8):1322-1332.

Figure Legend

Figure 1. 1-Phenyl-2-thiourea (PTU) induces aberrant autophagosome and autolysosome formation in zebrafish embryos. (**A**) Representative bright field images showing the pigmentation of 2 days post fertilization (dpf) zebrafish embryo treated with E3 (Control, CTRL) and 0.003% (200 μM or 1X) 1-Phenyl-2-thiourea in E3 (PTU) from around 1 dpf. Scale bar, 0.5mm; (**B**) Western blot results showing the dose-dependent accumulation of Lc3-I, Lc3-II, and degradation of sqstm1/p62 proteins in various-dose PTU-treated zebrafish embryos compared with CTRL. Mean relative ratio of Lc3-I:α-tubulin (α-tub), Lc3-II:α-tub, and sqstm1:α-tub were presented under the bands. 50 embryos were collected per group for three independent experiments. One-way ANOVA was applied and significant increase ($p<0.05$) in Lc3-I:α-tub and Lc3-II:α-tub was detected under PTU treatments compared with control in a dose-dependent manner, while significant decrease ($p<0.05$) was found in sqstm1:α-tub in 2X and 4X-treatment compared with CTRL. (**C**) Schematic diagram showing the position (periderm or basal epidermal cells above the eye) of imaging. Representative images from nine Tg(GFP-Lc3) zebrafish embryos treated with PTU and stained with LysoTracker from three independent experiments were shown. Three independent areas were selected from individual animals and the relative number of GFP-Lc3+, LysoTracker+ and Merged (GFP-Lc3+ and LysoTracker+) puncta per cell was quantified. Red arrow head, GFP-Lc3+ and LysoTracker+ puncta. **, $p<0.01$ compared with CTRL. Scale bar, 10 μm (Merged), 5 μm (Enlarged). (**D**) Schematic diagram showing the position (cells in midbrain) of imaging. The relative number of GFP-Lc3+, LysoTracker+ and Merged (GFP-Lc3+ and LysoTracker+) puncta per cell in neurons of midbrain was counted based on Z-Stack (10 layers out of 100 layers) image. Representative images of nine Tg(GFP-Lc3) zebrafish embryos treated with PTU

and/or 3-methyladenine (3-MA) and stained with LysoTracker from three independent experiments were shown. Red arrow head, GFP-Lc3+ and/or LysoTracker+ puncta. *, $p<0.05$, **, $p<0.01$ compared with CTRL; $^{\#\#}$, $p<0.01$ compared with PTU. Scale bar, 40 μm (Merged), 6 μm (Enlarged).

Figure 2. PTU elevates autophagic flux in zebrafish embryos. (**A**) Schematic diagram showing the position (dorsal view of skin on head) of imaging. Autophagic flux was detected by using GFP-LC3-RFP-LC3ΔG probe. The ratio of GFP-LC3:RFP-LC3ΔG was calculated based on mean fluorescent intensity in the selected area. Representative images of nine zebrafish embryos from three independent experiments were shown. Red arrow head, GFP-LC3+ and RFP-LC3ΔG+ puncta. **, $p<0.01$ compared with control (CTRL). Scale bar, 100 μm. (**B**) Schematic diagram showing the position (midbrain) of imaging. GFP-LC3 and RFP-LC3ΔG co-localized puncta were detected in midbrain of 24 hpf embryo treated PTU from 6 hpf. Red arrow head, GFP-LC3+ and/or RFP-LC3ΔG+ puncta. Scale bar, 100 μm. Representative images of nine zebrafish embryos from three independent experiments were shown. (**C**) Western blot results showing the level of Lc3-I and Lc3-II proteins in CTRL and PTU groups treated with chloroquine (CQ). Mean relative ratio of Lc3-II:α-tubulin (α-tub) was presented under the bands. 50 embryos were collected per group for three independent experiments. Two-way ANOVA with Tukey post hoc was applied and significant increase ($p<0.05$) in Lc3-II:α-tub was detected between PTU and PTU+CQ but not CTRL and CTRL+CQ. (**D**) Schematic diagram showing the position (cells in midbrain) of imaging. The relative number of GFP-Lc3+ and LysoTracker-, GFP-Lc3- and LysoTracker+, and GFP-Lc3+ and LysoTracker+ puncta per cell in neurons of midbrain was counted based on Z-Stack (10 layers out of 100 layers) images.

Representative images of nine Tg(GFP-Lc3) zebrafish embryos stained with LysoTracker treated with PTU and/or CQ from three independent experiments were shown. Red arrow head, GFP-Lc3+ and/or LysoTracker+ puncta. **, $p<0.01$ compared with CTRL; $^{\#\#}$, $p<0.01$ compared with PTU. Scale bar, 40 μm and 3 μm (Enlarged).

Figure 3. Aberrant autophagosome and autolysosome formation in tyr^{Mut} zebrafish embryos. (**A**) Representative bright field images showing the pigmentation of 2 days post fertilization (dpf) zebrafish embryo injected with *tyr* gRNA+Cas9 protein (tyr^{Mut}) and their sibling control (CTRL). Scale bar, 0.5 mm. (**B**) Western blot results showing the level of Lc3-I and Lc3-II proteins in CTRL and tyr^{Mut} groups treated with chloroquine (CQ). Mean relative ratio of Lc3-II:α-tubulin (α-tub) was presented under the bands. 50 embryos were collected per group for three independent experiments. Two-way ANOVA with Tukey post hoc was applied and significant increase ($p<0.05$) of Lc3-I and Lc3-II were detected in tyr^{Mut} compared with CTRL while no significant differences ($p>0.05$) in Lc3-II:α-tub were detected between tyr^{Mut} treated with CQ and tyr^{Mut}. (**C**) Schematic diagram showing the position (periderm or basal epidermal cells above the eye) of imaging. Representative images of nine tyr^{Mut} Tg(GFP-Lc3) zebrafish embryos stained with LysoTracker from three independent experiments were shown. Three independent areas were selected from individual animals and the relative number of GFP-Lc3+, LysoTracker+ and Merged (GFP-Lc3+ and LysoTracker+) puncta per cell were quantified. Red arrow head, GFP-Lc3+ and LysoTracker+ puncta. *, $p<0.05$ compared with CTRL. Scale bar, 10 μm (Merged), 5 μm (Enlarged). (**D**) Schematic diagram showing the position (cells in midbrain) of imaging. The relative number of GFP-Lc3+ and LysoTracker-, GFP-Lc3- and LysoTracker+, and GFP-Lc3+ and LysoTracker+ puncta per cell in neurons of midbrain were counted based on Z-Stack

(10 layers out of 100 layers) images. Representative images of nine tyr^{Mut} Tg(GFP-Lc3) zebrafish embryos treated CQ and stained with LysoTracker from three independent experiments were shown. Red arrow head, GFP-Lc3+ and/or LysoTracker+ puncta. **, $p<0.01$ compared with CTRL; $^{\#\#}$, $p<0.01$ compared with tyr^{Mut}. Scale bar, 40 μm (Merged), 3 μm (Enlarged).

Figure 4. L-tyrosine but not autophagic modulators restores melanogenesis in PTU-treated zebrafish embryos. (**A**) Representative bright field images showing the pigmentation of 2 days post fertilization (dpf) zebrafish embryo treated with autophagic modulators, including E3, dimethyl sulfoxide (DMSO), chloroquine (CQ), 3-methyladenine (3-MA), rapamycin and L-tyrosine with or without PTU. Red arrow head, melanin shown in Enlarged. Scale bar, 0.5 mm. (**B**) Schematic diagram showing the position (cells in midbrain) of imaging. The relative number of GFP-Lc3+, LysoTracker+ and Merged (GFP-Lc3+ and LysoTracker+) puncta per cell were counted based on Z-Stack (10 layers out of 100 layers) images. Representative images of nine Tg(GFP-Lc3) zebrafish treated with PTU, L-tyrosine, or PTU+L-tyrosine and stained with LysoTracker prior to imaging from three independent experiments were shown. Red arrow head, GFP-Lc3+ and/or LysoTracker+ puncta. **, $p<0.01$ compared with CTRL; $^{\#\#}$, $p<0.01$ compared with L-tyrosine. Scale bar, 40 μm (Merged), 6 μm (Enlarged).

Figure 1

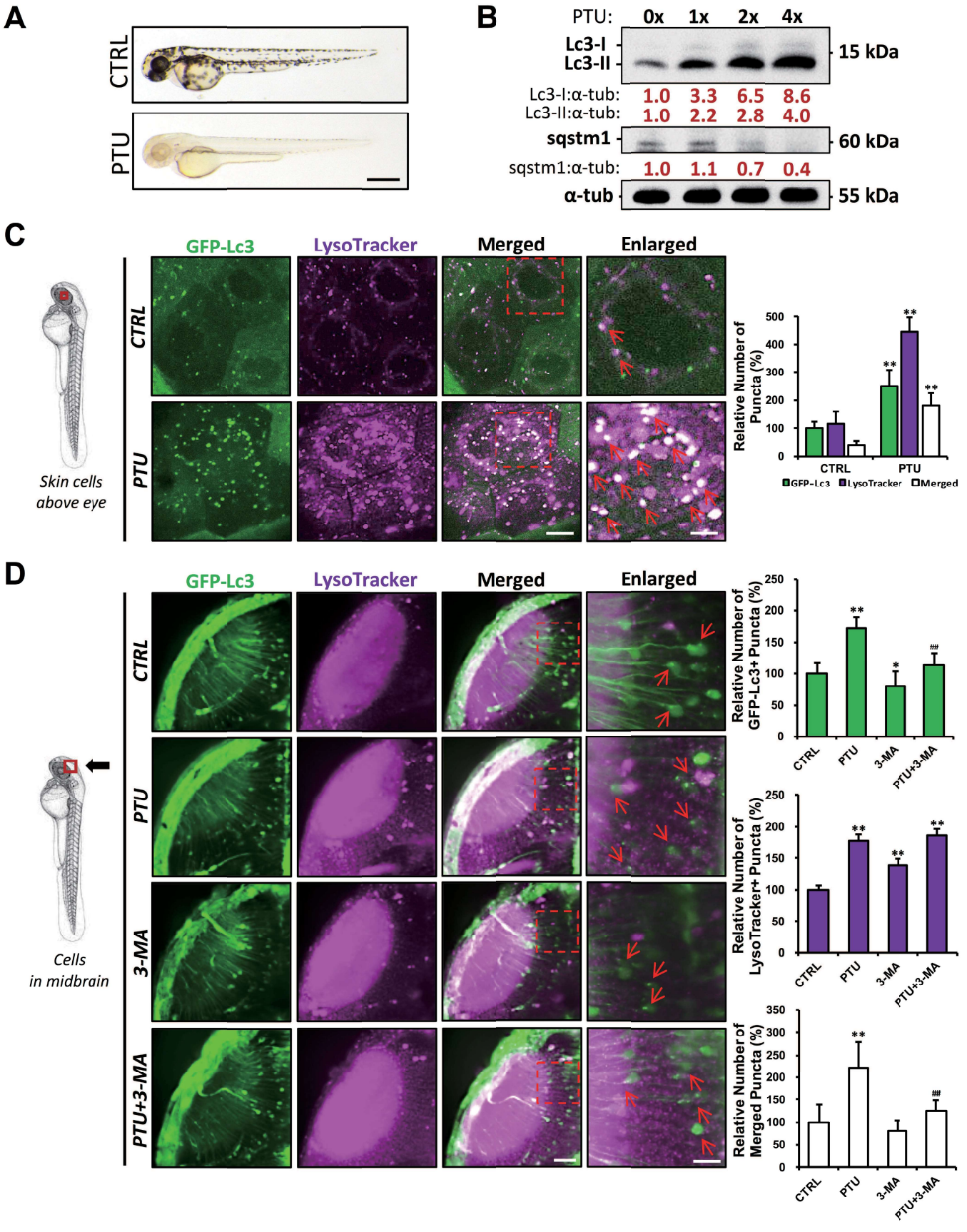
A
CTRL
PTU
B
PTU: 0x 1x 2x 4x
Lc3-I
Lc3-II
15 kDa
Lc3-I:α-tub: 1.0 3.3 6.5 8.6
Lc3-II:α-tub: 1.0 2.2 2.8 4.0
sqstm1
60 kDa
sqstm1:α-tub: 1.0 1.1 0.7 0.4
α-tub
55 kDa
C
GFP-Lc3
LysoTracker
Merged
Enlarged
CTRL
PTU
Skin cells above eye
Relative Number of Puncta (%)
CTRL
PTU
GFP-Lc3
LysoTracker
Merged
D
GFP-Lc3
LysoTracker
Merged
Enlarged
CTRL
PTU
3-MA
PTU+3-MA
Cells in midbrain
Relative Number of GFP-Lc3+ Puncta (%)
Relative Number of LysoTracker+ Puncta (%)
Relative Number of Merged Puncta (%)
CTRL
PTU
3-MA
PTU+3-MA

Figure 2

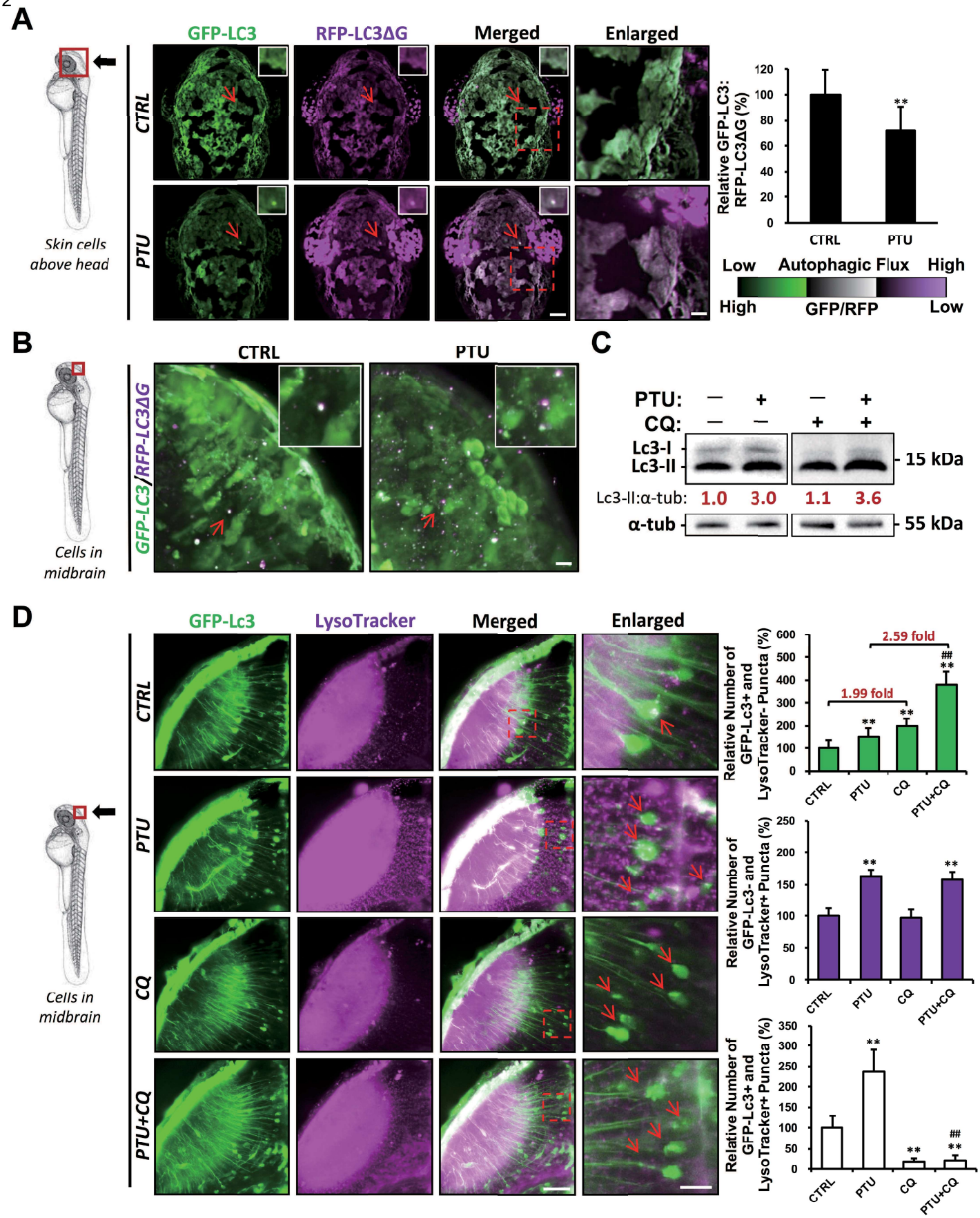
A
GFP-LC3
RFP-LC3ΔG
Merged
Enlarged
CTRL
PTU
Skin cells above head
Relative GFP-LC3: RFP-LC3ΔG (%)
120
100
80
60
40
20
0
**
CTRL
PTU
Low
Autophagic Flux
High
High
GFP/RFP
Low
B
CTRL
PTU
GFP-LC3/RFP-LC3ΔG
Cells in midbrain
C
PTU:
CQ:
Lc3-I
Lc3-II
15 kDa
Lc3-II:α-tub:
1.0
3.0
1.1
3.6
α-tub
55 kDa
D
GFP-Lc3
LysoTracker
Merged
Enlarged
CTRL
PTU
CQ
PTU+CQ
Cells in midbrain
Relative Number of GFP-Lc3+ and LysoTracker- Puncta (%)
2.59 fold
1.99 fold
600
500
400
300
200
100
0
**
##
CTRL
PTU
CQ
PTU+CQ
Relative Number of GFP-Lc3- and LysoTracker+ Puncta (%)
250
200
150
100
50
0
Relative Number of GFP-Lc3+ and LysoTracker+ Puncta (%)
350
300
250
200
150
100
50
0

Figure 3

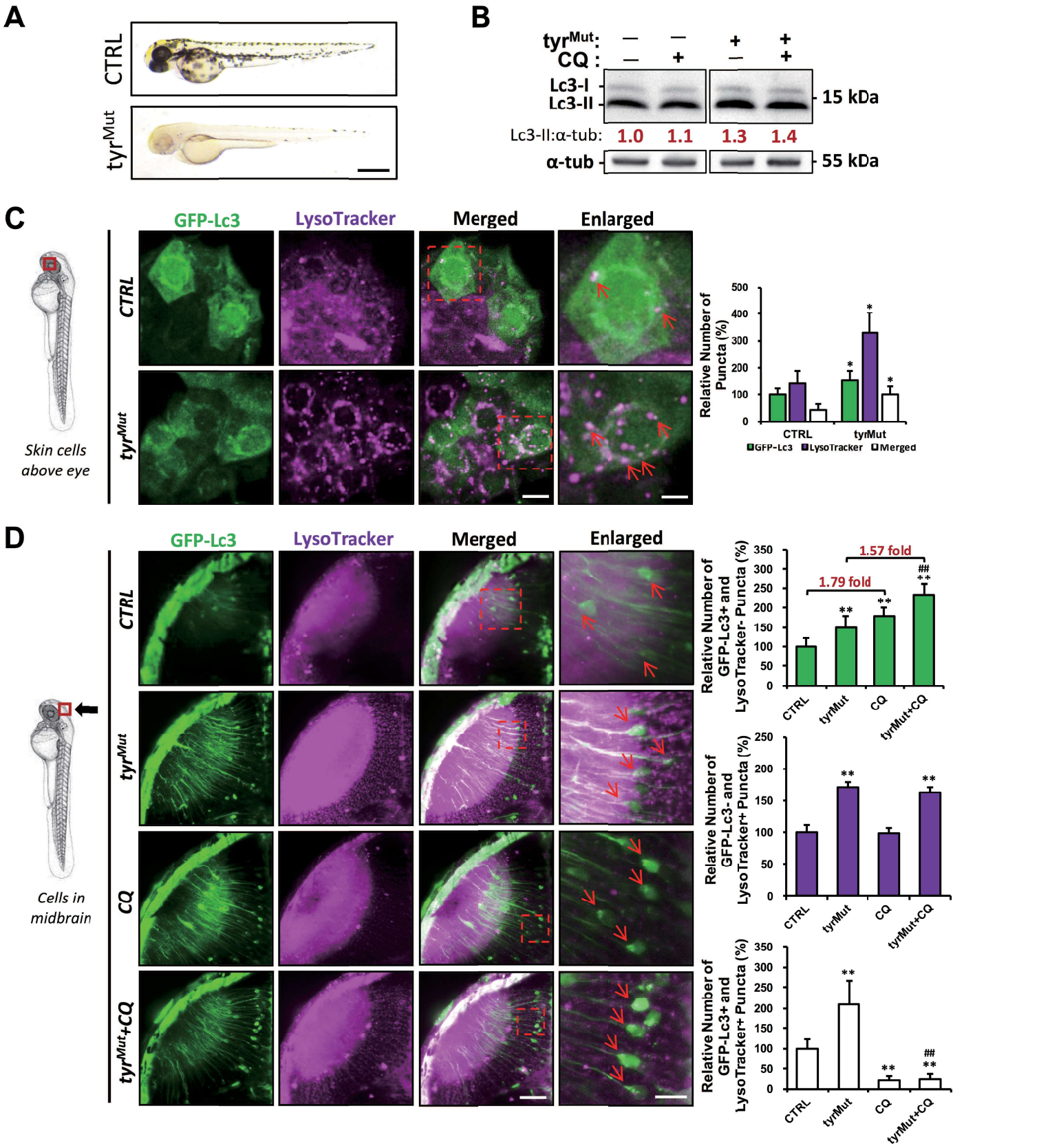
A
CTRL
tyrMut
B
tyrMut:
CQ :
Lc3-I
Lc3-II
15 kDa
Lc3-II:α-tub:
1.0
1.1
1.3
1.4
α-tub
55 kDa
C
GFP-Lc3
LysoTracker
Merged
Enlarged
CTRL
tyrMut
Skin cells above eye
Relative Number of Puncta (%)
CTRL
tyrMut
GFP-Lc3
LysoTracker
Merged
D
GFP-Lc3
LysoTracker
Merged
Enlarged
CTRL
tyrMut
CQ
tyrMut+CQ
Cells in midbrain
Relative Number of GFP-Lc3+ and LysoTracker- Puncta (%)
1.79 fold
1.57 fold
Relative Number of GFP-Lc3- and LysoTracker+ Puncta (%)
Relative Number of GFP-Lc3+ and LysoTracker+ Puncta (%)

Figure 4

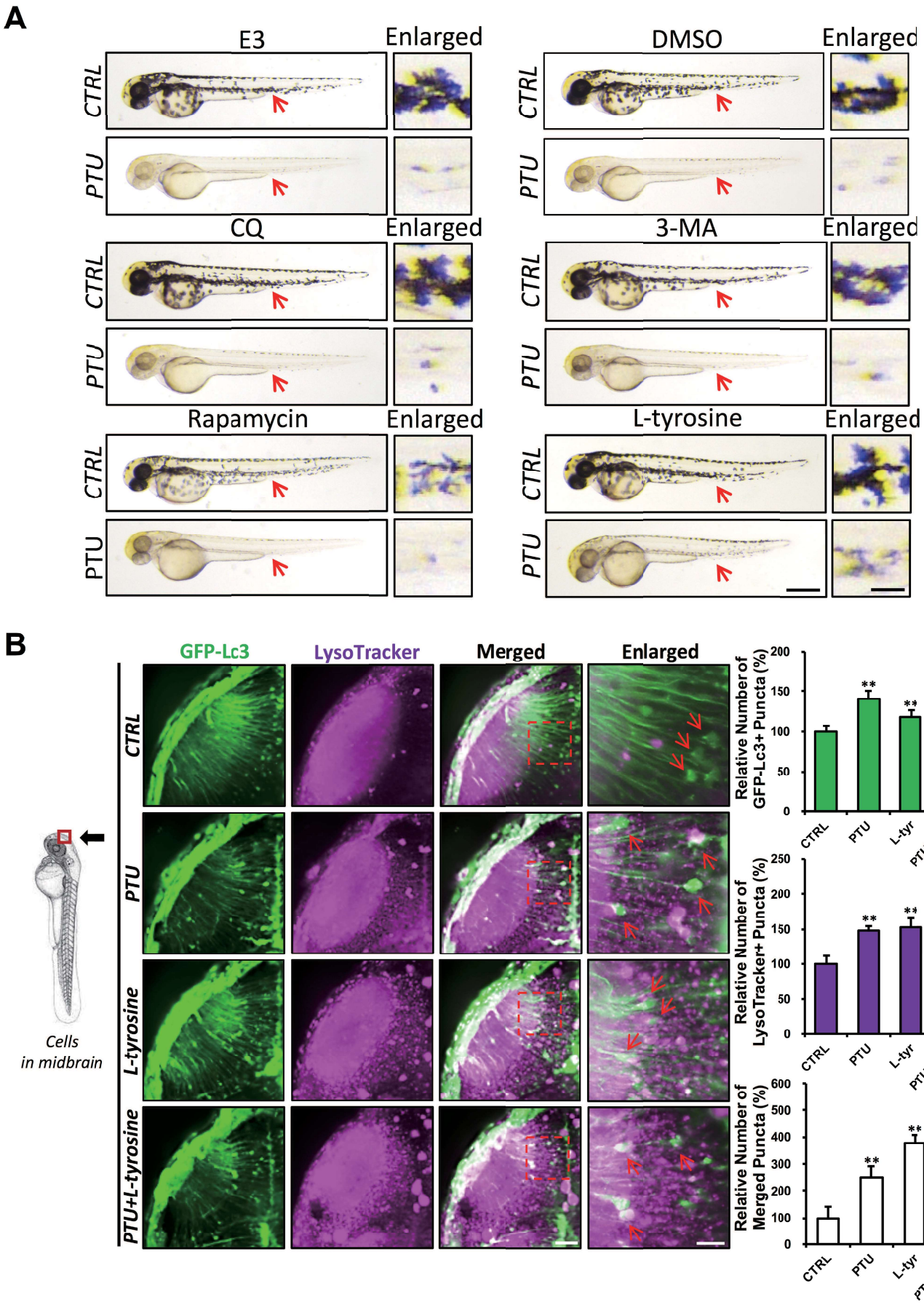
A
E3
Enlarged
DMSO
CQ
3-MA
Rapamycin
L-tyrosine
CTRL
PTU
B
GFP-Lc3
LysoTracker
Merged
Enlarged
Cells
in midbrain
PTU+L-tyrosine
Relative Number of GFP-Lc3+ Puncta (%)
Relative Number of LysoTracker+ Puncta (%)
Relative Number of Merged Puncta (%)
L-tyr
PTU+L-tyr

Supplementary Figures

Figure S1

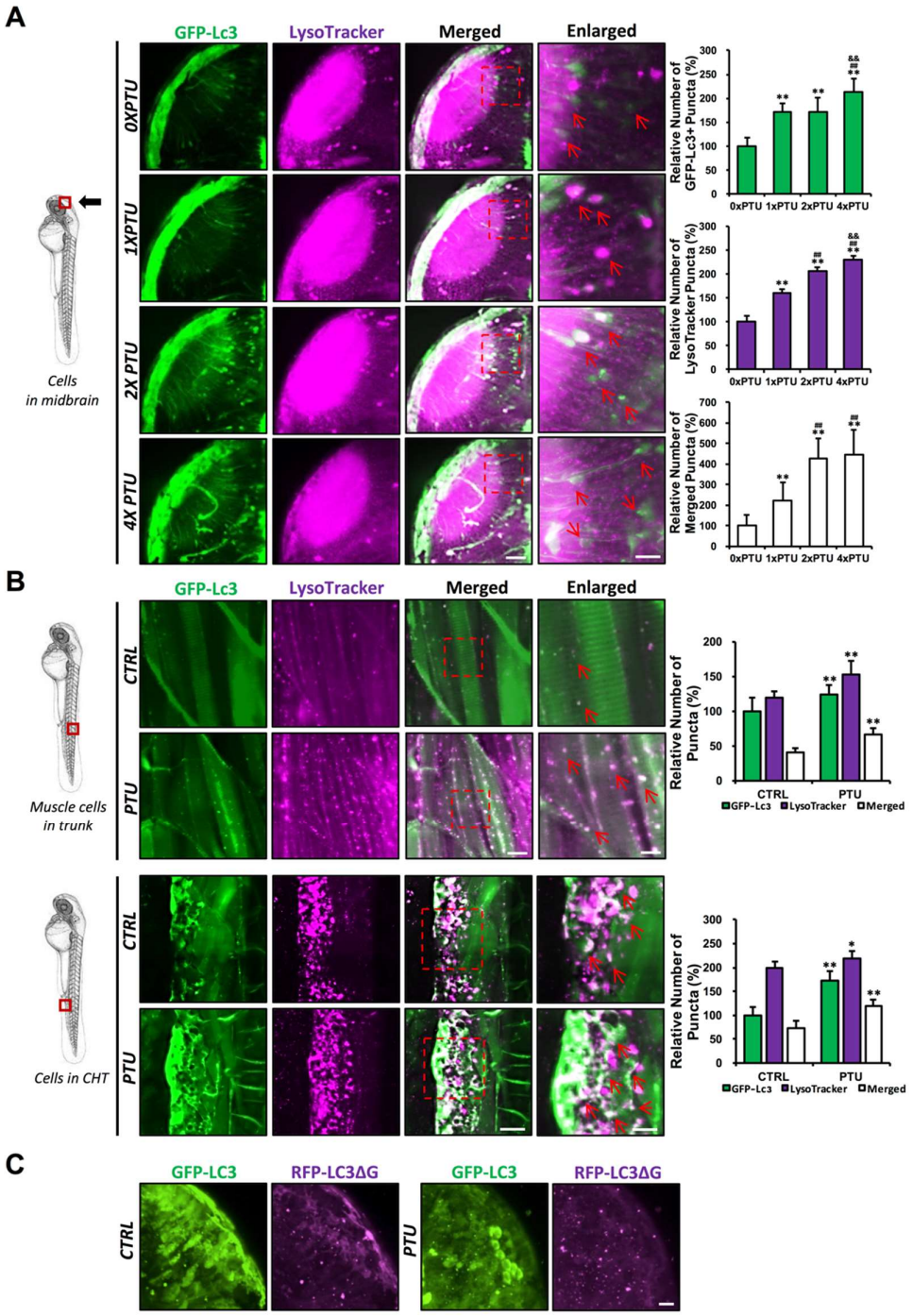

Figure S1. 1-phenyl-2-thiourea (PTU) induces a dose-dependent autophagosome and autolysosome formation in various tissues of zebrafish embryos. (**A**) Schematic diagram showing the position (cells in midbrain) of imaging. The relative number of

GFP-Lc3+, LysoTracker+, and Merged (GFP-Lc3+ and LysoTracker+) puncta per cell were counted based on Z-Stack (10 layers out of 100 layers) images. Representative images of nine Tg(GFP-Lc3) zebrafish treated with various doses of PTU (0X, 1X, 2X, and 4X) and stained with LysoTracker prior to imaging from three independent experiments were shown. Red arrow head, GFP-Lc3+ and/or LysoTracker+ puncta. **, $p<0.01$ compared with 0XPTU; $^{\#\#}$, $p<0.01$ compared with 1XPTU; $^{\&\&}$, $p<0.01$ compared with 2X PTU. Scale bar, 40 μm (Merged), 6 μm (Enlarged). (**B**) *upper panel*: Schematic diagram showing the position (muscle cells in the trunk) of imaging. The number of GFP-Lc3+, LysoTracker+ and Merged (GFP-Lc3+ and LysoTracker+) puncta per muscle cell in trunk were counted. Representative images for nine Tg(GFP-Lc3) zebrafish embryos treated with PTU and stained with LysoTracker from three independent experiments were shown. Red arrow head, GFP-Lc3+ and/or LysoTracker+ puncta. **, $p<0.01$ compared with control (CTRL). Scale bar, 10 μm (Merged), 5 μm (Enlarged). *Lower panel*: Schematic diagram showing the position caudal hematopoietic tissue (CHT) of imaging. The number of GFP-Lc3+, LysoTracker+, and Merged (GFP-Lc3+ and LysoTracker+) puncta per cell in caudal hematopoietic tissue (CHT) were counted. Representative images for nine Tg(GFP-Lc3) zebrafish treated with PTU and stained with LysoTracker prior to imaging from three independent experiments were shown. Red arrow head, GFP-Lc3+ and/or LysoTracker+ puncta. **, $p<0.01$ compared with control (CTRL). (**C**) GFP-LC3+ and RFP-LC3ΔG+ cytoplasm and puncta in midbrain of 24 days post fertilization (dpf) GFP-LC3-RFP-LC3ΔG probe-injected embryo treated PTU from 6 hpf. Scale bar, 150 μm.

Figure S2

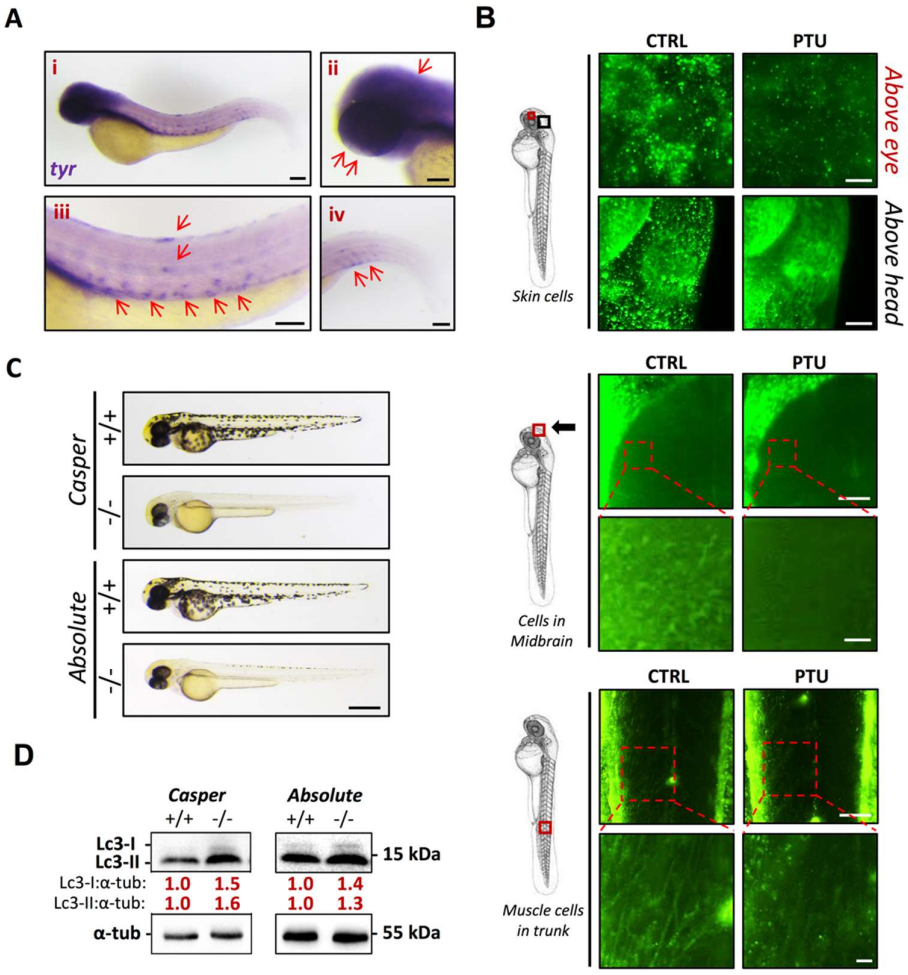

Figure S2. Spatial expression of tyrosinase in wild-type and aberrant autophagic activity in *Casper* and *Absolute* zebrafish embryos. (**A**) Representative whole-mount in situ hybridization images showing tyrosinase (*tyr*) expression in bleached 3 days post fertilization (dpf) wildtype zebrafish embryo. Expression of *tyr* was observed in the whole body of zebrafish embryo (i), largely in the eye and head (or brain) (ii), melanocytes (Red arrow) and trunk (or muscle) (iii), and caudal hematopoietic tissue (CHT) (iv), Red arrow head, *tyr*+ signal. Scale bar, 100 μm; (**B**) Representative immunostaining images showing tyrosinase protein expression in the skin cells (higher panel), midbrain (middle panel) and muscle cells (lower panel) of bleached zebrafish embryos treated with or without PTU. Scale bar, 5 μm (skin cell above eye); 200 μm (skin cell above head); 50 μm (midbrain); 10 μm (enlarged midbrain); 50 μm (muscle); 10 μm (enlarged muscle); (**C**) Representative bright field images showing the

pigmentation of 2 dpf homozygous (-/-) *Casper* and *Absolute* zebrafish embryo and their wildtype (+/+) siblings. Scale bar, 0.5 mm; (**D**) Western blot results showing accumulation of Lc3-I and Lc3-II in homozygous (-/-) *Casper* or *Absolute* zebrafish embryos compared with their wildtype (+/+) siblings. Mean relative ratio of Lc3-I:α-tubulin (α-tub) and Lc3-II:α-tub was presented under the bands. 50 embryos were collected per group for 3 independent experiments. Paired t-test was applied and significant increase ($p<0.05$) in Lc3-I:α-tub and Lc3-II:α-tub of homozygous *Casper* and *Absolute* zebrafish embryos compared with their wildtype siblings were detected.

Figure S3

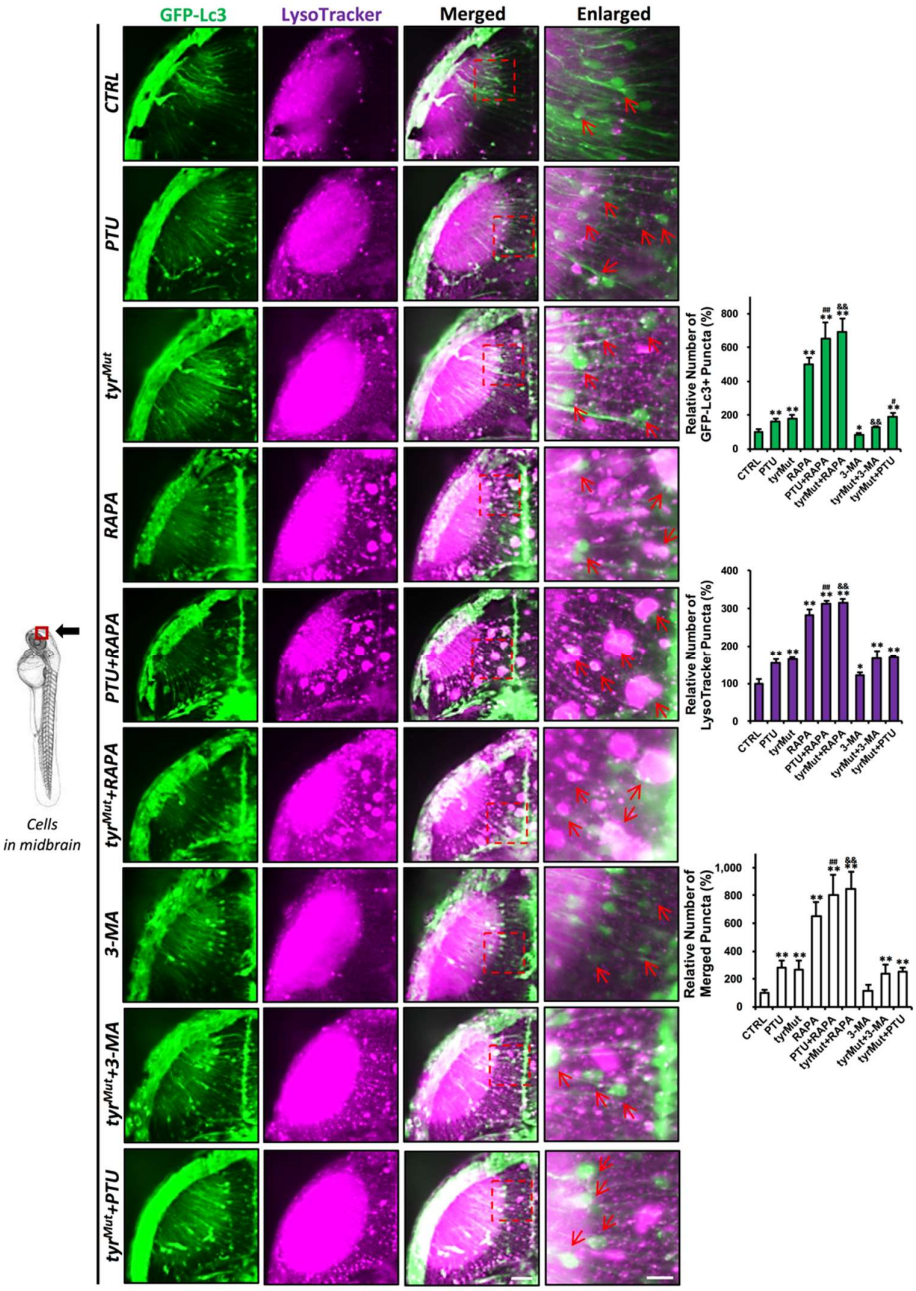

Figure S3. Autophagic modulators modulates autophagy in PTU-treated and tyr^{Mut} zebrafish embryos. Schematic diagram showing the position (cells in midbrain) of imaging. The number of GFP-Lc3+, LysoTracker+ and Merged (GFP-Lc3+ and LysoTracker+) puncta per cell in neuron of midbrain were counted based on Z-Stack (10 layers out of 100 layers) images. Representative images of nine Tg(GFP-Lc3) zebrafish injected with *tyr* gRNA (**tyr^{Mut}**) and/or treated with PTU and various

autophagic modulators, including rapamycin and 3-methyladenine (3-MA), and stained with LysoTracker prior to imaging from three independent experiments were shown. Red arrow head, GFP-Lc3+ and/or LysoTracker+ puncta. *, $p<0.05$, **, $p<0.01$ compared with control (CTRL); $^{\#}$, $p<0.05$, $^{\#\#}$, $p<0.01$ compared with PTU; &&, $p<0.01$ compared with t**yr**$^{\mathbf{Mut}}$. Scale bar, 40 μm (Merged), 6 μm (Enlarged).

Supplementary materials and methods [1]

Whole-mount in situ hybridization.

Partial cDNA sequence of tyrosinase (*tyr*) was amplified by PCR with specific primers (tyr-F: GATCGAGAGCGATGGCCTTT and tyr-R: GGGCACCATGAAGTATCCGT). PCR product was then cloned into pGEM-T-easy vector (Promega, A1360) and subsequently applied as template to generate an antisense digoxigenin (DIG) labeled RNA probe via using DIG RNA Labelling Kit (Roche, 11277073910). Whole-mount in situ hybridization (WISH) was performed as described previously [1].

Whole-mount immunostaining.

Dechorionated embryos were fixed in 4 % paraformaldehyde (PFA) (Sigma-Aldrich, P6148) at 4 °C overnight and then dehydrated and rehydrated with gradient concentration ethanol in phosphate buffered saline (VWR, 97062-732) plus Tween 20 (PBST). After washing with PBST, embryo washed with Tris buffer (150 mM Tris-HCl, pH 9.0) and equilibrated in Tris buffer at 70 °C for 15 min. Afterward, embryos were penetrated with pre-chilled acetone at -20 °C for 20 min and then blocked with 10 % normal goat serum (NGS) and 2 % bovine serum albumin (BSA) in phosphate buffered plus Triton X-100 (PBT) for 4 h at 4 °C. Embryos were probed with anti-Tyrosinase (Santa Cruz Biotechnology, sc-20035) primary antibody diluted in 2 % NGS and 2 % BSA in PBT at 4 °C overnight and then incubated with Alexa Fluor 488-labeled goat anti-mouse IgG secondary antibody (Invitrogen, A-11029) in 2 % NGS and 2 % BSA in PBT in dark for 2 h at room temperature. After washing, embryos were stored in dark at 4 °C before imaging.

Reference

1. Ma AC, Ward AC, Liang R, et al. The role of jak2a in zebrafish hematopoiesis. Blood. 2007;110(6):1824-1830.